H_∞ Repetitive Control for Pickup Head Flying Height in Near-Field Optical Disk Drives

J. W. Chen and T. S. Liu

***Abstract*—The slider of a flying pickup head in a near-field optical disk drive has to fly at a stable height above the disk surface. An air bearing force between the slider and optical disk is affected by disk rotation speed and deformation, which represent low-frequency periodic disturbance to the slider. The repetitive control is adopted in this study to eliminate the periodic disturbance. H_∞ control inherited with robust properties can deal with model uncertainty and disturbances. Therefore, to solve model uncertainty and disturbance, this study designs a repetitive controller cascaded by an H_∞ controller. The proposed controller is validated by experimental results.**

***Index Terms*—Air bearing, H_∞ control, near-field optical disk drive, pickup head, repetitive control.**

I. Introduction

In order to overcome the diffraction limit of conventional optical disk drives and substantially increase data storage capacity and density, near-field optical disk drives remain to be realized. Enhancing control performance to stabilize the fly height of the pickup head in near-field optical disk drives is demanded. To achieve accurate and stable flying height, this study develops an H_∞ repetitive controller, which unifies characteristics of H_∞ control into repetitive control. A multiplicative uncertainty H_∞ design method is employed in feedback control, which fulfills disturbance and uncertainty rejection requirements and guarantees closed-loop stability. However, the desired position command and tracking response generally are periodic signals due to disk vibration. Therefore, a time-delay positive feedback controller is incorporated, thereby repetitive control offers a competent approach to position tracking, since it can deal with a large number of harmonics simultaneously, even with several disturbances at different frequencies.

II. H_∞ Control

In this study, a pickup head model is identified by using a laser Doppler interferometer. Its transfer function is obtained as

$$\mathrm{G(s)} = \frac{3.805\times10^{7}\mathrm{s}^2 + 4.394\times10^{9}\mathrm{s} + 4.033\times10^{14}}{\mathrm{s}^4+1203\mathrm{s}^3+1.047\times10^{8}\mathrm{s}^2+2.657\times10^{10}\mathrm{s}+4.235\times10^{14}}. \quad (1)$$

Manuscript received August 28, 2004. This work was supported by the National Science Council, Taiwan, R.O.C., under Grant NSC93-2752-E009-009-PAE.

The authors are with the Department of Mechanical Engineering, National Chiao Tung University, Hsinchu 30010, Taiwan, R.O.C. (e-mail: plato.me88g@nctu.edu.tw; tsliu@mail.nctu.edu.tw).

Digital Object Identifier 10.1109/TMAG.2004.842018

In order to deal with system uncertainty, this study designs an H_∞ controller. First, consider a reference model of $\mathrm{G(s)}$ with variance 10%. Since the reference model for $\mathrm{G(s)}$ has six variances due to two zeros and four poles, both upper and lower bounds lead to $2^6 = 64$ transfer functions. Based on (1), a model of uncertainty can be written as

$$\mathrm{G}_\Delta(\mathrm{s}) = \frac{\mathrm{num(s)}}{\mathrm{den(s)}} \quad (2)$$

where

$$\mathrm{num(s)} = 3.805\times10^{7}\mathrm{s}^2 + 4.394\times10^{9}(1+0.1\Delta_1)\mathrm{s} + 4.033\times10^{14}(1+0.1\Delta_2)$$

$$\mathrm{den(s)} = \mathrm{s}^4 + 1203(1+0.1\Delta_3)\mathrm{s}^3 + 1.047\times10^{8}(1+0.1\Delta_4)\mathrm{s}^2 + 2.657\times10^{10}(1+0.1\Delta_5)\mathrm{s} + 4.235\times10^{14}(1+0.1\Delta_6)$$

and $\Delta_1, \Delta_2, \Delta_3, \Delta_4, \Delta_5$, and $\Delta_6 \in [-1, 1]$. Define the unstructured uncertainty boundary error as $\Delta(j\omega) = \mathrm{G}_\Delta(j\omega) - \mathrm{G}(j\omega)$. A Bode diagram for $\Delta(j\omega)$ is shown in Fig. 1. According to the small gain theorem, all perturbations must be under the upper bound [1]. Therefore, dealing with the upper-bound contour, which is constructed based on Fig. 1, this study defines a weighting function

$$\mathrm{W}_2(\mathrm{s}) = \frac{2.894\times10^{4}\mathrm{s}^2 + 4.426\times10^{7}\mathrm{s} + 1.916\times10^{10}}{3.805\times10^{7}\mathrm{s}^2 + 4.394\times10^{9}\mathrm{s} + 4.033\times10^{14}} \quad (3)$$

and a multiplicative uncertainty $\Delta_\mathrm{m}(\mathrm{s}) = (\mathrm{G}_\Delta(\mathrm{s}) - \mathrm{G(s)})/(\mathrm{G(s)})$. It requires that $|\Delta_\mathrm{m}(\mathrm{jw})| \leqq |\mathrm{W}_2(\mathrm{jw})|$ [1]. An H_∞ optimization problem is to find a stabilizing controller $\mathrm{K}_\infty(\mathrm{s})$ such that $\|\mathrm{SW}_1\|_\infty < 1, \|\mathrm{RW}_2\|_\infty < 1, \|\mathrm{TW}_3\|_\infty < 1$ where S, R, and T denote $(\mathrm{I} + \mathrm{GK}_\infty)^{-1}$, $\mathrm{K}_\infty(\mathrm{I} + \mathrm{GK}_\infty)^{-1}$, and $\mathrm{GK}_\infty(\mathrm{I} + \mathrm{GK}_\infty)^{-1}$, respectively. The performance of the weighting function $\mathrm{W}_1(\mathrm{s})$ is prescribed as a low-pass filter that weights heavily at low frequency to achieve good tracking performance. Moreover, the weighting function $\mathrm{W}_3(\mathrm{s})$ is used to represent the frequency content of the sensor noise. Hence, $\mathrm{W}_3(\mathrm{s})$ is prescribed as

$$\mathrm{W}_3(\mathrm{s}) = \frac{3.553\times10^{8}}{\mathrm{s}^2 + 2.665\times10^{4}\mathrm{s} + 3.553\times10^{8}}. \quad (4)$$

The function $\mathrm{W}_1(\mathrm{s})$ is prescribed as

$$\mathrm{W}_1(\mathrm{s}) = \frac{3.948\times10^{7}}{\mathrm{s}^2 + 1.194\times10^{4}\mathrm{s} + 3.948\times10^{7}}. \quad (5)$$

The H_∞ controller can be derived using (1) and (3)–(5) to become

$$\mathrm{K}_\infty(\mathrm{s}) = \frac{\mathrm{k}_\infty\mathrm{num(s)}}{\mathrm{k}_\infty\mathrm{den(s)}} \quad (6)$$

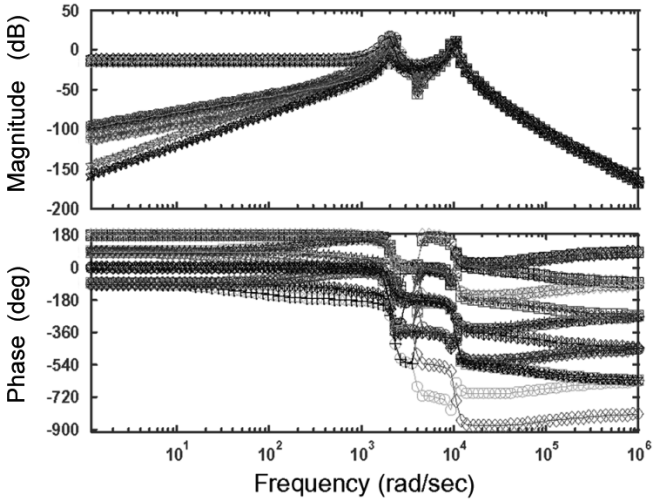

Fig. 1. Bode diagram of unstructured uncertainty boundary error $\Delta(j\omega)$.

where

$$\begin{aligned}
K_\infty num(s) &= 2.038\times10^{6}s^{9} + 8.446\times10^{10}s^{8} \\
&\quad + 1.799\times10^{15}s^{7} + 2.123\times10^{19}s^{6} \\
&\quad + 1.883\times10^{23}s^{5} + 1.328\times10^{27}s^{4} \\
&\quad + 2.776\times10^{30}s^{3} + 1.585\times10^{34}s^{2} \\
&\quad + 9.762\times10^{36}s + 4.38\times10^{40} \\
K_\infty den(s) &= s^{10} + 1.828\times10^{5}s^{9} + 1.679\times10^{10}s^{8} \\
&\quad + 8.509\times10^{14}s^{7} + 2.58\times10^{19}s^{6} \\
&\quad + 2.504\times10^{23}s^{5} + 1.257\times10^{27}s^{4} \\
&\quad + 5.127\times10^{30}s^{3} + 1.748\times10^{34}s^{2} \\
&\quad + 2.718\times10^{37}s + 7.447\times10^{40}.
\end{aligned}$$

For robust tracking, instead of utilizing precise models with controller, this study has developed a robust H_∞ controller. The system model parameters are allowed to be rough.

III. Repetitive Control

For the slider of a flying pickup head in a near-field optical disk drive, tracking performance is influenced by disturbances with periodic components appearing at a known fundamental frequency corresponding to the disk speed and its higher harmonics. Repetitive controllers [2] can improve tracking performance by rejecting periodic disturbances. However, in selecting the bandwidth of a low-pass filter in the repetitive controller, which determines steady-state error and system stability, most existing approaches require trials and error. Further, in case the plant has uncertainties, to guarantee system stability the bandwidth is likely to be limited. As a result, the steady-state error does not decrease within a specified bound anymore. Any periodic signal with period L can be generated by a time-delay system with an appropriate initial function [3]. The system has infinitely many poles on the imaginary axis. The closed-loop systems model is $\exp(-Ls)/(1-\exp(-Ls))$. Consider a repetitive control system with the model $a(s) + \exp(-Ls)/(1 - \exp(-Ls))$ depicted in Fig. 2 where $a(s)$ in the feedforward path is a proper stable rational function. $P(s)$, a transfer function for the compensated plant, is a proper stable rational function. Y_0 and Q_0 denote Laplace transforms of responses to initial conditions of $P(s)$ and $\exp(-Ls)$, respectively. It follows from Fig. 2 that the error is written as

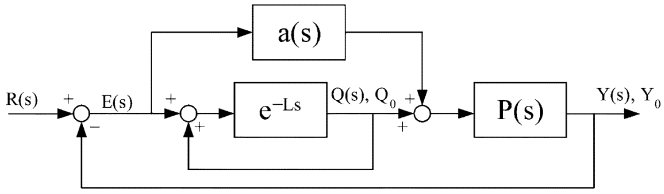

Fig. 2. Repetitive control system.

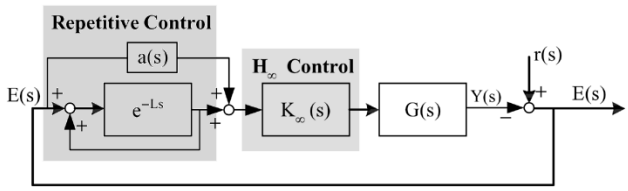

Fig. 3. Block diagram of H_∞ repetitive control.

$$E = \exp(-Ls)(I+aP)^{-1}[I+(a-1)P]E+(I+aP)^{-1}D_0 \quad (7)$$

where $D_0 = (1 - \exp(-Ls))(R - Y_0) - PQ_0$. The convergence condition or stability condition for the repetitive control system can be examined by considering the BIBO stability for the equivalent system described by (7) with an aid of the small gain theorem. An exogenous input $\mathcal{L}^{-1}[(I + aP)^{-1}D_0]$ is an $\mathcal{L}_2$ function under the assumption of the asymptotic stability of $(I + aP)^{-1}P$ where $\mathcal{L}^{-1}$ denotes an inverse Laplace transform. According to the above assumption, concerning Fig. 2 there are two sufficient conditions for stability of repetitive control systems:

$$[I + a(s)P(s)]^{-1}P(s) \in \text{proper and stable} \quad (8)$$

$$\|(I + a(s)P(s))^{-1}[I + (a(s) - 1)P(s)]\|_\infty < 1. \quad (9)$$

This work designs a repetitive controller to cascade an H_∞ controller as depicted in Fig. 3, where the H_∞ controller employs $K_\infty(s)$ and plant model (1). According to (8) and (9), this study designs $a(s) = (0.000\,397\,9s + 1)/(0.000\,265\,3s + 1)$. Fig. 4 compares open-loop Bode diagrams of the plant $G(s)$ with and without the H_∞ repetitive controller, which compensates for 90 Hz and its multiples.

IV. Experiment

Bode diagrams for the pickup head, pickup head with an H_∞ controller, and pickup head with an H_∞ repetitive control are shown in Fig. 4. The dotted line denotes the Bode diagram of the pickup head and the dash-dotted line the pickup head with an H_∞ controller, in which the H_∞ controller eliminates two resonant peaks in the dotted line and increases insensitivity. Low sensitivity tolerates model uncertainty of the pickup head.

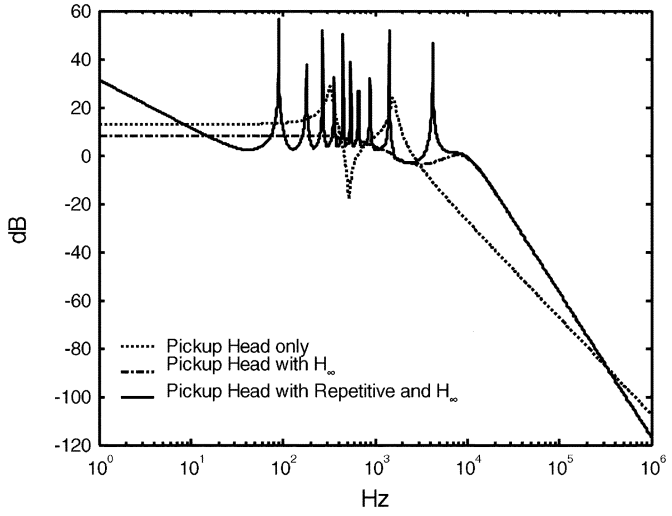

Fig. 4. Bode diagrams of pickup head with and without controller.

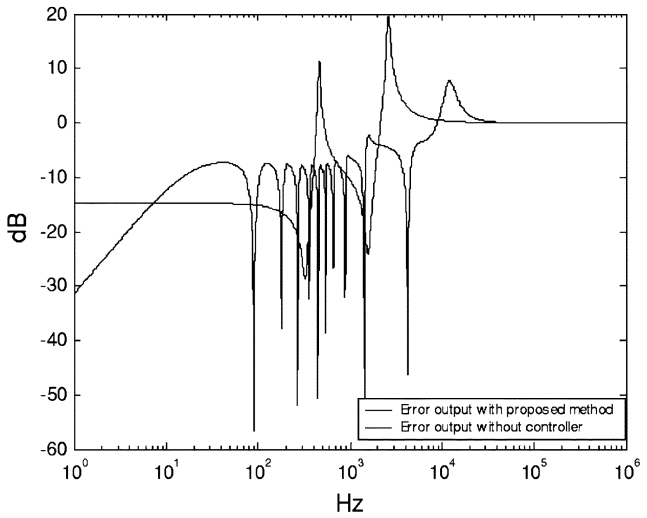

Fig. 5. Bode diagram of output error with and without controller.

In order to reduce disk flutter disturbance, the H_∞ controller cascades a repetitive controller based on disturbances frequency of disk vibration and results in the solid line in Fig. 4. It exhibits many peaks that are multiples of 90 Hz corresponding to the disturbance frequency. Repetitive control enhances the system sensitivity at specific frequencies.

The Bode diagram for $E(s)$ is shown solid line in Fig. 5. The solid line in Fig. 5, disturbances of 90 Hz and its multiples are not sensitivity. That is, the specific disturbances frequency can be eliminated. The dot line is not compensated with any controller.

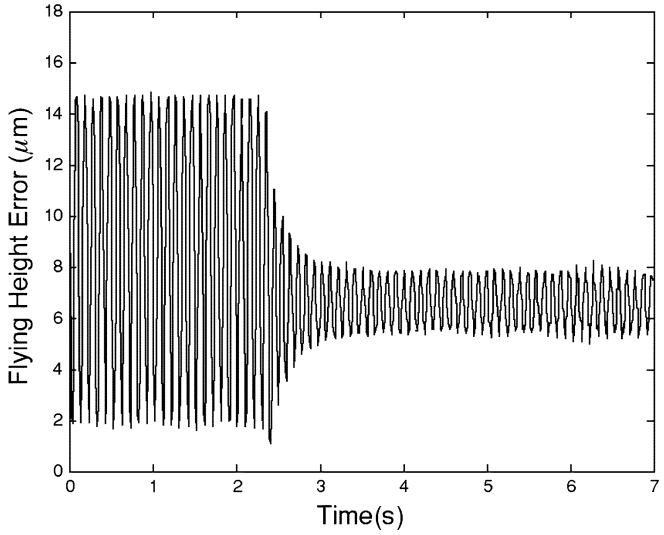

Fig. 6. Experimental results.

According to measurement, the disk flutter signal can be decomposed into 11 modes of the form

$$\begin{aligned} r(t) = {} & 23\sin(2\pi 90t) + 14.84\sin(2\pi 180t) \\ & + 1.06\sin(2\pi 270t) + 1.34\sin(2\pi 360t) \\ & + 0.35\sin(2\pi 450t) + 0.16\sin(2\pi 540t) \\ & + 0.25\sin(2\pi 630t) + 0.23\sin(2\pi 718t) \\ & + 0.26\sin(2\pi 808t) + 0.11\sin(2\pi 898t) \\ & + 0.15\sin(2\pi 988t). \end{aligned}$$

Using the proposed H_∞ repetitive control method, experimental results of disturbance input with $r(t)$ are depicted in Fig. 6. Before 2.4 s the main frequency of reference input is a sinusoid at 90 Hz mixed with its multiples. Hence, the period L of the repetitive controller is prescribed as $1/90$ s. As a consequence, the present controller reduces the flying height error to 12% of the original one.

V. Conclusion

The proposed control method incorporates repetitive control to reject periodic disturbances. An H_∞ design method has been used to ensure that the pickup head performs effectively within stability region. As a result, flying height error arising from disk flutter is significantly reduced in experiments.

References

[1] K. Zhou and J. C. Doyle, *Essentials of Robust Control*. Upper Saddle River, NJ: Prentice-Hall, 1998.

[2] S. Hera and Y. Yamamoto, "Stability of repetitive control systems," in *Proc. IEEE 24th Conf. Decision and Control*, 1985, pp. 326–327.

[3] S. Hera, Y. Yamamoto, T. Omata, and M. Nakano, "Repetitive control system: A new type servo system for periodic exogenous signals," *IEEE Trans. Automat. Contr.*, vol. 37, no. 7, pp. 659–668, Jul. 1988.